International Journal on Advanced Science Engineering Information Technology

Vol.13 (2023) No. 5
ISSN: 2088-5334

Assessing the Accuracy of Land Use Classification Using Multi-spectral Camera From LAPAN-A3, Landsat-8 and Sentinel-2 Satellite: A Case Study in Probolinggo-East Java

Ega Asti Anggari [a], Agus Herawan [a,*], Patria Rachman Hakim [a] , Agung Wahyudiono [a], Sartika Salaswati [a], Elvira Rachim [a] , Zylshal Zylshal [b]

[a] *Research Center for Satellite Technology, National Research and Innovation Agency, Bogor, 16310, Indonesia*
[b] *Remote Sensing Ground Station, National Research and Innovation Agency, Pare-pare, 91131, Indonesia*
Corresponding author: [*]agus112@brin.go.id

***Abstract*— The LAPAN-A3 is the third microsatellite generation developed by the Research Center for Satellite Technology. The satellite can be used for land classification, agriculture monitoring, drought monitoring, and land use change. This study aims to classify land use and land cover in the research area. The main image used is LAPAN-A3; the compared images are Landsat-8 and Sentinel-2. Three images were taken on the same day and selected on cloud-free terms. The classification process starts with determining the region of interest (ROI) and the class. The classification is divided into six classes: water, forests, rice fields, settlements, open land, and coastal areas. The classification technique uses supervised learning with the maximum likelihood method. This study used Landsat 8 and Sentinel-2 data to compare the results obtained from LAPAN-A3. The accuracy test results for the LAPAN-A3 and Landsat-8 are 84.7042% and 0.783, respectively. While the accuracy test of LAPAN-A3 and Sentinel-2 is 72.2313%, the kappa value is 0.6394. The classification of two comparisons is quite accurate, with an accuracy of more than 70%. The LA3 classification successfully identifies water and coastal areas. The producer and accuracy is substantiated by comparing the results with both Landsat-8 and Sentinel-2 satellite data, which exhibit an accuracy rate exceeding 85%. Finally, LAPAN-A3 has great potential for classifying land use and land cover when compared to Landsat 8 and Sentinel-2 images, but future research should increase the number of datasets and vary the research area to improve the results.**

***Keywords*— Multispectral; LAPAN-A3; Kappa value; Probolinggo; maximum likelihood.**

Manuscript received 15 Jan. 2023; revised 29 Apr. 2023; accepted 22 Aug. 2023. Date of publication 31 Oct. 2023.

I. INTRODUCTION

LAPAN-A3 is a microsatellite developed by the Satellite Technology Center which has a resolution of 15 m and can be used for various purposes [1]. Since orbiting 2016, many parties have used it for monitoring rice fields, drought, oil spill detection, and hydrological analysis [2]–[4]. Most of the utilization is used in agriculture and land use, which is associated with the spectral that can be captured by the camera [5], [6]. Land use and land cover classification is among the most widely applied satellite images [7]–[9]. This data can be used for policy-making, administration, and business [10]. Classification can be done with supervised or unsupervised techniques. The supervised technique requires training data [11].

Meanwhile, the unsupervised technique works with groups of image pixels into several classes based on certain statistical calculations without specifying the training data used by the computer as a reference for classifying [12]. Accuracy calculation is an important process in classification [13]. Overall accuracy compares each correct pixel from the data used with reference data [14]. The reference data is assumed to have the same information as the actual data on the surface. With this accuracy calculation, the error value in the data can be known, and the quality of the classification results can be revealed [15]. Landsat-8 and Sentinel-2 are remote sensing satellites widely used for earth monitoring [16]–[18]. The data, which can be downloaded for free, is widely used by various groups of people. Satellites that have medium-resolution cameras (30 m for Landsat-8 and 10 m for Sentinel-2) are widely used for land use and land cover classification

[19], [20]. LAPAN-A3 satellite landcover classification has been carried out in research [21]. A tree algorithm was used in this research. The availability of sensors that can record wavelengths, more specifically, there is an added value in determining the number of classification classes. This study aims to classify land use and cover in the study area, namely Probolinggo, East Java. The main data used is the LAPAN-A3 image. The classification results will be compared with the results of the Landsat 8 and Sentinel-2 classifications. The results are a classification map with the accuracy test results in the form of accuracy values and kappa values.

II. Material and Method

A. Study Area

The data for the study are LAPAN-A3 multi-spectral camera, Landsat 8, and Sentinel-2 satellites. Three images were taken on the same day, September 28, 2018. The study area is in the Probolinggo district, East Java, with the coordinates of latitude $7^0$33' S- $7^0$51'S and longitude $113^0$16'E - $113^0$30'E. Area of this study is shown in Fig. 1.

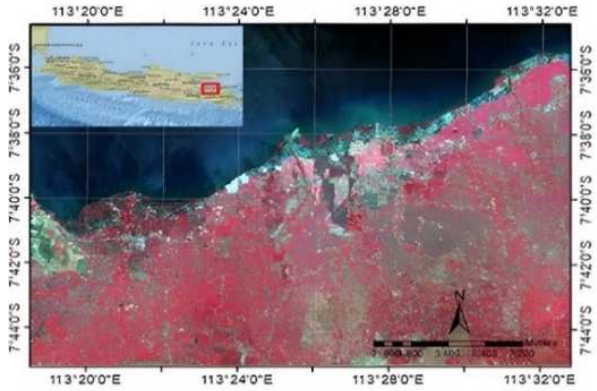

Fig. 1 Map of the study area, Probolinggo (East Java)

Data is selected on cloud-free terms and retrieved on the same day. The LA3 data was obtained by an independent acquisition by the LAPAN Center using the LAPAN-A3 satellite. After creating an account, OLI and Sentinel-2 images can be downloaded for free on the United States Geological Survey (USGS) website. Data information can be seen in Table 1.

TABLE I
RESEARCH DATA

Satellite	Date (yyyy/mm/dd)	Resolution	Cloud cover (%)
LAPAN-A3 (LA3)	2018/09/28	15 m	0
LANDSAT-8 (OLI)	2018/09/28	30 m	0
SENTINEL-2	2018/09/28	10 m	0

B. Preprocessing

The preprocessing stage at LA3 (Level L0) is done by correcting the vignetting so that an image with uniform brightness is obtained radiometric [22]. Followed by a co-registration process that produces a blur-free image [23][24]. Then, proceed with the georeferencing process [25]. The image is projected onto the WGS 84 datum, the Universal Transverse Mercator. The georeferencing process was carried out between LA3 and OLI, with OLI as a reference. The LA3 data that is ready to be processed is the L1B level data.

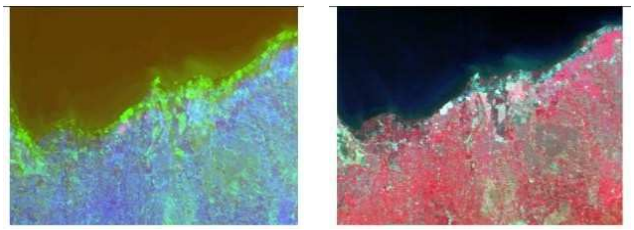

(a). L0 Level (b). L1 Level

Fig. 2 LAPAN-A3 (LA3) image

The image processed in the next step is formed into the Nir-Red-Green band formation. The preprocessing stage for the OLI composite band was made on band 543. Meanwhile, for Sentinel-2, a composite is made on band 843. Furthermore, the OLI image is used for reference during the georeferencing process on LA3 and Sentinel-2. The differences between L0 level and L1B level can be seen in Fig. 2.

C. Workflow Study

The first step in this research is to choose the Region of Interest (ROI) for the Probolinggo area. Classes are determined by using high-resolution image data from Google Earth as a reference. Six categories of water, forest, rice fields, settlements, open land, and coastal areas are used to categorize the land that is utilized. The next step is to create training data, which is necessary when using supervised classification techniques. Thirty-eight training data sets have been created with polygons that are spread throughout the image data. The placement and number of polygons are assumed to represent the entire research area. Data training and data validation are only carried out with visual interpretation on Google Earth without surveying the field because the data used is archive data. The methodology of research is shown in Fig. 3.

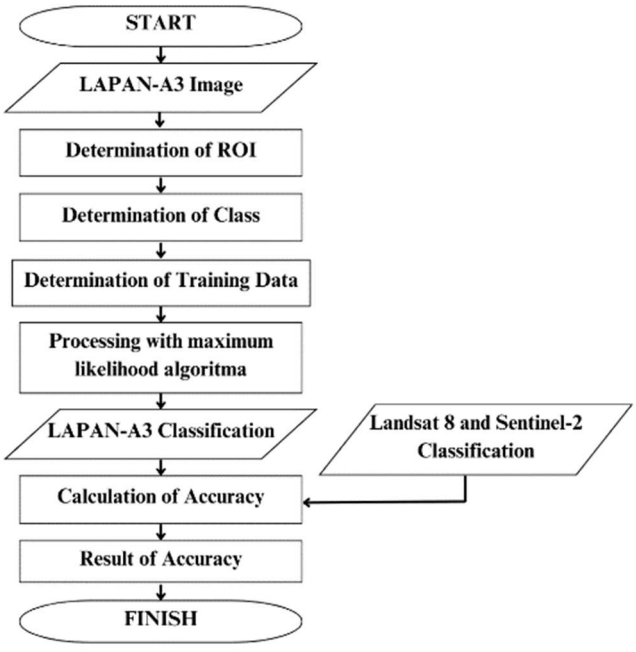

Fig. 3 Research Methodology

D. Classification Using Maximum Likelihood

Maximum likelihood is a method of estimating the probability distribution parameters by maximizing the probability function so that, based on the statistical model, the assumptions of the observed data are most likely. Maximum likelihood classification is based on the probability that a pixel belongs to a certain class [26]–[28]. Based on the Bayesian Equation, an Algorithm to calculate the weighted distance or likelihood A of the unknown X vector measurement based on the known class M_c.

$$A = ln(a_c) - |0.5\, ln(|Cov_c|)| - [0.5(X - M_c)]T(Cov_c - 1)(x - M_c) \quad (1)$$

A is the weighted distance, c is a specific class, $X$is the measurement vector of the candidate pixels, M_c is the average vector of the sample class c, a_c is the possible percentage of several candidate pixels that are members of class c , Cov_c is the covariance matrix of the pixels in the class c sample, $|Cov_c|$ is the determinant of Cov_c, Cov_c-1 is the inverse of Cov_c, ln is the natural logarithm of the function, and T is the transpose function.

E. Accuracy Testing

The accuracy test is a crucial stage. This stage can tell the user how accurate the classification results are. In general, accuracy is displayed in the form of an error matrix. An error matrix is a square array of rows and columns containing pixel information, a collection of pixels or polygons [29]–[31]. The column shows the reference data, while the row shows the classification results from the remote sensing data. Overall accuracy is obtained from the correct number of pixels divided by the total pixels [32]–[34]. Producer accuracy is the number of correct pixels in a category divided by the number of pixels in the reference data (column total) category. This accuracy producer calculates the probability that the reference pixel is correctly classified and is a measure of the omission error. User accuracy is obtained from the number of correct pixels in a category divided by the number of pixels classified in the category (total rows) [35]–[37].

In the accuracy test, the Kappa value is usually displayed as the result of a statistical KHAT analysis, although there are other ways to show the accuracy results. Kappa values range from 0 to 1, indicating total disagreement, and 1 indicating total agreement [38]–[40]. The analysis results will be meaningless if the matrix is not generated correctly. Factors that need to be considered in the accuracy test are surface data, classification scheme, spatial autocorrelation, sample size, and sampling scheme [41]–[43].

III. Results and Discussion

A. Land Use and Land Cover Classification

The images used in this study are LA3, OLI, and Sentinel-2, taken on the same day, September 28, 2018. This study uses data on the same day to minimize differences in atmospheric effects that can affect data quality [44]. The LA3 data has gone through the radiometric and geometric correction stages. The LA3, OLI, and Sentinel-2 data used the Nir-Red-Green band for classification. Fig. 4. shows the research area.

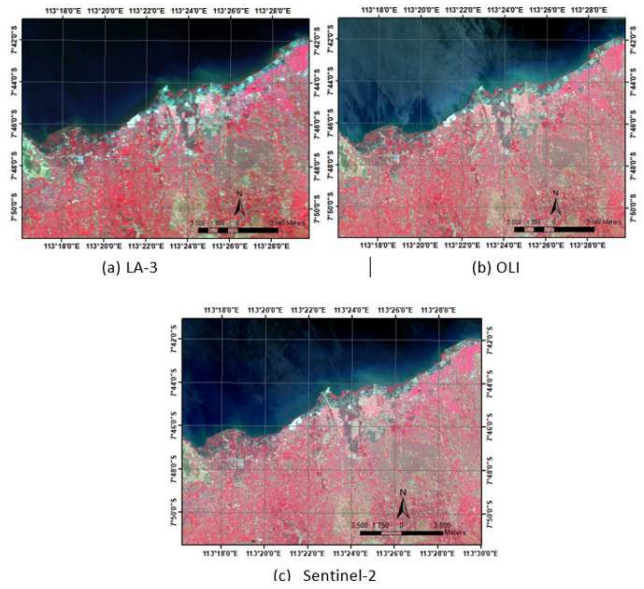

Fig. 4 Images used for land use and cover classification.

Fig. 5. shows a map of land use and cover classification results on LA3, OLI, and Sentinel-2 images. Classification using the maximum likelihood method. Visually, the classification results are not so far between LA3 and OLI. Waters, coasts, and rice fields have a similar pattern. Meanwhile, forests, settlements, and open land have similar patterns, although there are differences in some areas. The classification results on sentinel-2 waters, coastal and open land have a pattern like other images. The paddy fields that dominate the LA3 and OLI images do not occur in the results of the sentinel-2 classification because the results of the classification of residential and forest areas are wider.

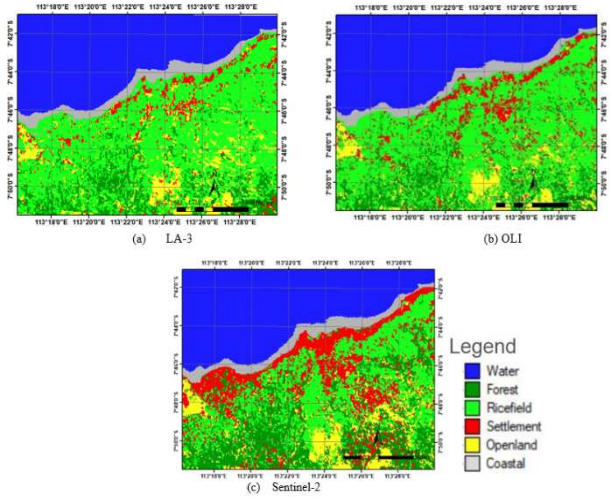

Fig. 5 Land cover and Land use Classification Map

The results of the LA3 classification show that most of the research area is rice fields, with an area of 222.5057 km2. Water is the second dominating land cover, with an area of 160.3319 km^2. The rest of the land cover is forest, settlements, open land, and coastal areas with an area of 46.5162 km^2, 21.3582 km^2, 36.9741 km^2, and 22.0980 km^2, respectively. The total research area itself is 509.7841 km^2. More details can be seen in Table II.

TABLE II
LAND COVER AREA AS A RESULT OF LA-3, OLI AND SENTINEL-2 BY CLASS

Land use	LA3 Area (Km^2)	OLI Area (Km^2)	Sentinel-2 Area (Km^2)	Absolute Difference A3-Oli (Km^2)	Absolute Difference A3-Sentinel2 (Km^2)
Water	160.3319	161.6383	161.2624	1.3064	0.9305
Forest	16.5162	54.2612	94.8379	7.7450	48.3217
Ricefield	222.5057	206.0667	116.1646	16.4390	106.3410
Settlement	21.3582	34.6251	72.1113	13.2669	50.7531
Open Land	36.9741	31.6892	43.4275	5.2849	6.4534
Coastal	22.0980	21.5036	21.9804	0.5944	0.1176
Total	509.7841	509.7841	509.7841		

The results of the OLI classification have the same area as the LA3 and Sentinel-2 area, i.e., 5,097,841 km^2. Rice fields dominate the land, covering an area of 2,060,667 km^2. The waters have a wide coverage of 1,616,383 km^2. Followed by forests, settlements, open land, and coastal areas with an area of 542,612 km^2, 346,251 km^2, 316,892 km^2, and 215,036 km^2.

The difference in area between LA3 and OLI obtained the lowest value, namely the coastal area of 0.5,944 km2. This illustrates that the results of the classification of coastal areas on LA3 also mostly produce coastal classifications in OLI. The highest area difference is rice fields with 164,390 km^2, which illustrates an area of 164,390 km^{2,} resulting in the classification of rice fields in LA3, but in OLI, the classification is not rice fields.

The results of the Sentinel-2 classification show that the total water area is 1,612,624 km^2, as is the land cover that dominates the research area. Followed by rice fields with an area of 1,161,646 km^2. Forests, settlements, and open land have an area of 948,379 km^2, 721,113 km^2, and 434,275 km^2, respectively. The coast has the narrowest area, with a value of 219,804 km^2.

The difference in area between LA3 and Sentinel-2 has a large enough difference for forest land cover, rice fields, and settlements with an area of 483,217 km^2, 1,063,410 km^2, and 507,531 km^2, respectively. This shows an area of 483,217 km^{2,} which is classified as forest in Sentinel-2, but in LA3 it results in a non-forest classification. An area of 106.3410 km^2 is classified as rice fields in LA3, but Sentinel-2 results in a non-rice field classification. An area of 507,531 km^2 is a settlement classification in Sentinel-2, but on LA3, it results in a non-settlement classification.

B. Accuracy Statement

Tables III and IV present the results of the accuracy calculation in the research area. The calculation of accuracy uses a confusion matrix approach by comparing the LA3 image with the reference image (OLI and Sentinel 2). The last column shows the reference data. The row shows the classification results from the remote sensing data. The diagonals show the correct classification results. Pixels that are not classified in the correct class are not on the diagonal and assign values to different classes between the reference and remote sensing data classes.

Table III shows the accuracy of LA3 against OLI. This study's accuracy value is above 85% in the water, rice fields, and coastal classes. In that class, only a few errors were read into another class. Forest and open land have 65.81% and 63.97% accuracy, respectively. Most of the errors in this class are read as rice fields.

This indicates confusion in classifying forest and open land so that they are read in OLI as rice fields. The smallest accuracy in settlements was with a value of 39.28%. The error in this class is read as 40.47% rice fields and 19.91% open land. There are errors in settlements because the residential pixels are too small, so they are read into another class adjacent to the residential pixels.

A blur effect on LA3 causes the ability to separate spectra in the classification process to be less than optimal. The calculation results show an overall accuracy of 84.70425% with a kappa coefficient of 0.783. The number of classes in the classification was made due to the limitations of the existing bands in LISA.

TABLE III
CALCULATION OF ACCURACY LA3 AGAINST OLI FORM LAND USE AND LAND COVER CLASSIFICATION IN PROBOLINGGO – EAST JAVA

Class	Water	Forest	Rice filed	Settlement	Open Land	Coastal	Total
Water	**98.68**	0.00	0.00	0.00	0.00	3.86	31.45
Forest	0.00	**65.81**	4.42	0.23	5.11	0.00	9.12
Rice field	0.14	31.77	**88.83**	40.57	21.97	4.52	43.65
Settlement	0.03	1.29	2.01	**39.28**	8.96	0.12	4.19
Open Land	0.00	1.12	4.46	19.91	**63.97**	0.03	7.25
Coastal	1.15	0.00	0.28	0.02	0.00	**91.47**	4.23
Total	100.00	100.00	100.00	100.00	100.00	100.00	100.00

Table IV shows the accuracy of LA3 against Sentinel-2. This study found more than 85% accuracy in the water, rice fields, and coastal classes. In that class, only a few errors were read into another class. Forest and open land have an accuracy of 44.30% and 55.33%, respectively. The error in this class is read as rice fields. This is due to confusion in classifying forest and open land so that it is read in Sentinel-2 as rice fields. Settlements have an accuracy of only 19.73%. The majority of them read as rice fields, with a value of 67.71%, and open land, with a value of 11.22%.in settlements, because residential pixels are too small, they are read into another class adjacent to residential pixels. The overall accuracy of LA3 against Sentinel-2 shows a value of 72.2313% with a kappa value of 0.6394.

A previous study showed a moderate value in the spectral correlation between LA3 and Sentinel-2. Radiometric correction to eliminate atmospheric effects has not been applied to the image, resulting in uneven illumination in LA3. This results in reducing the accuracy of the classification results.

TABLE IV
CALCULATION OF ACCURACY LA3 AGAINST SENTINEL-2 FORM LAND USE AND LAND COVER CLASSIFICATION IN PROBOLINGGO – EAST JAVA

Class	Water	Forest	Rice filed	Settlement	Open Land	Coastal	Total
Water	**98.97**	0.00	0.00	0.00	0.00	3.29	31.45
Forest	0.00	**44.30**	2.39	0.51	3.12	0.00	9.12
Rice field	0.00	51.49	**93.40**	67.71	33.48	6.24	43.65
Settlement	0.00	1.64	1.76	**19.73**	8.07	0.14	4.19
Open Land	0.00	2.12	2.44	11.22	**55.33**	0.05	7.25
Coastal	1.03	0.00	0.00	0.83	0.00	**90.28**	4.23
Total	100.00	100.00	100.00	100.00	100.00	100.00	100.00

Table V shows the producer accuracy and user accuracy values. The producer accuracy value is inversely proportional to the omission error. The producer accuracy value indicates the probability that the actual land cover has been correctly assigned to the land cover category. The user accuracy value is inversely proportional to the commission error. The user accuracy value indicates the perspective of the user's map, referring to the truth in the field.

It can be seen that the LA3-OLI producer accuracy for water, paddy, and coastal classes is quite high, with a value above 85%. Accuracy between 85% and 50% is in forest and open land classes. While the accuracy is below 50%, that is the settlement class. Producer accuracy for residential classes is low due to the error pixels being read into the paddy field and open land classes in the reference image. Regarding user accuracy, LA3-OLI above 85% is water and coastal class. Accuracy ranges between 85% and 50% in the forest, paddy fields, settlement, and open land classes.

TABLE V
CALCULATION OF PRODUCER ACCURACY AND USER ACCURACY

Class	Producer Accuracy La3-Oli (%)	User Accuracy La3-Oli (%)	Producer Accuracy La3-Sentinel (%)	User Accuracy La3-Sentinel (%)
Water	98.68	99.48	98.97	99.55
Forest	65.81	76.77	44.30	90.33
Ricefield	88.83	82.27	93.40	48.76
Settlement	39.28	63.68	19.73	66.61
Open Land	63.97	54.82	55.33	64.98
Coastal	91.47	89.01	90.28	89.80

For LA3-Sentinel accuracy, producer accuracy above 85% is found in water, rice fields, and coastal classes. Open land grade accuracy ranges between 85% and 50%. While the accuracy in the forest and settlement classes is less than 50%, in terms of user accuracy, LA3-Sentinel is above 85% in water, forest, and coastal. Accuracy between 85% and 50% is based on settlements and open land. The accuracy below 50% is in the rice field class. The accuracy value obtained is caused by the specifications and quality of each image and the user's factor in creating the training area. The formation of an over-segmented area causes a decrease in the accuracy value.

The process of creating training data is required for supervised classification techniques. Training data sets have been generated using polygons distributed across image data, assuming that these polygons represent the entire research area. The training and validation process involves visual interpretation on Google Earth. However, it is suggested to incorporate survey data from the field to validate the actual conditions on the ground.

IV. CONCLUSION

Classification of land use and land cover in the study area, namely Probolinggo, East Java, has been carried out using LAPAN-A3 image data as the main data. The results of the classification match the results of the Landsat 8 and Sentinel-2 classifications. The LA3 classification successfully identifies water bodies and coastal areas. The producer and user accuracy are substantiated by comparing the results with both OLI and Sentinel-2 satellite data, exhibiting an accuracy rate exceeding 85%. The results of the LAPAN-A3 and Landsat 8 overall accuracy tests are 84.7042%, and the kappa value is 0.783. While the overall accuracy test of LAPAN-A3 and sentinel-2 is feasible at 72.23%, the kappa value is 0.6,394. The limited number of bands in LA3 causes the classification list to be limited.

The lack of accuracy in LA3 is caused by several factors: the absence of a corrective atmosphere, a blur effect, and the training area. The classification of two comparisons is quite accurate, with an accuracy of more than 70%. Finally, LAPAN-A3 has great potential for classifying land use and land cover compared to Landsat 8 and Sentinel-2 images, but future research should increase the number of datasets and vary the research area to improve the results.

ACKNOWLEDGMENT

We thank the satellite operator team, including the mission planning and data processing team, who always give the best effort to keep the satellites healthy in orbit.

REFERENCES

[1] R. H. Triharjanto and P. R. Hakim, "Review of satellite technology development in Indonesian space agency based on its technical publications in 2012-2016," in *Proceedings of the International Astronautical Congress, IAC*, 2017, vol. 9.

[2] M. Mukhoriyah and D. Kushardono, "Application of Lapan A3 Satellite Data for The Identification of Paddy Fields Using Object Based Image Analysis (OBIA)," *Int. J. Remote Sens. Earth Sci.*, vol. 18, no. 1, 2021, doi: 10.30536/j.ijreses.2021.v18.a3378.

[3] P. M. Afgatiani *et al.*, "Assessing LAPAN-A3 Satellite with Line Imager Space Application (LISA) Sensor for Oil Spill Detection," *Int. J. Adv. Sci. Eng. Inf. Technol.*, vol. 12, no. 6, 2022, doi: 10.18517/ijaseit.12.6.16076.

[4] T. Getu Engida, T. A. Nigussie, A. B. Aneseyee, and J. Barnabas, "Land Use/Land Cover Change Impact on Hydrological Process in the Upper Baro Basin, Ethiopia," *Appl. Environ. Soil Sci.*, vol. 2021, 2021, doi: 10.1155/2021/6617541.

[5] A. K. Wijayanto, S. M. Yusuf, and W. A. Pambudi, "The Characteristic of spectral reflectance of LAPAN-IPB (LAPAN-A3) Satellite and Landsat 8 over agricultural area in Probolinggo, East Java," *IOP Conf. Ser. Earth Environ. Sci.*, vol. 284, no. 1, pp. 1–14, 2019, doi: 10.1088/1755-1315/284/1/012004.

[6] S. Zamzam, "Geological Controls and Prospectivity Mapping for Manganese Ore Deposits Using Predictive Modeling Comparison: An Integration of Outcrop and Remote Sensing Data, Sinai Microplate, Egypt," *J. Earth Sci.*, vol. 34, no. 2, 2023, doi: 10.1007/s12583-021-1583-z.

[7] G. Gopinath, N. Sasidharan, and U. Surendran, "Landuse classification of hyperspectral data by spectral angle mapper and support vector machine in humid tropical region of India," *Earth Sci. Informatics*, vol. 13, no. 3, 2020, doi: 10.1007/s12145-019-00438-4.

[8] Z. Yuan, J. Xu, Y. Wang, and B. Yan, "Analyzing the influence of land use/land cover change on landscape pattern and ecosystem services in the Poyang Lake Region, China," *Environ. Sci. Pollut. Res.*, vol. 28, no. 21, 2021, doi: 10.1007/s11356-020-12320-8.

[9] X. Y. Tong *et al.*, "Land-cover classification with high-resolution remote sensing images using transferable deep models," *Remote Sens. Environ.*, vol. 237, 2020, doi: 10.1016/j.rse.2019.111322.

[10] M. Chamling and B. Bera, "Spatio-temporal Patterns of Land Use/Land Cover Change in the Bhutan–Bengal Foothill Region Between 1987 and 2019: Study Towards Geospatial Applications and Policy Making," *Earth Syst. Environ.*, vol. 4, no. 1, 2020, doi: 10.1007/s41748-020-00150-0.

[11] T. Zhang, J. Su, Z. Xu, Y. Luo, and J. Li, "Sentinel-2 satellite imagery for urban land cover classification by optimized random forest classifier," *Appl. Sci.*, vol. 11, no. 2, 2021, doi: 10.3390/app11020543.

[12] W. Lv and X. Wang, "Overview of Hyperspectral Image Classification," *Journal of Sensors*, vol. 2020. 2020, doi: 10.1155/2020/4817234.

[13] A. Serwa and S. Elbialy, "Enhancement of classification accuracy of multi-spectral satellites' images using Laplacian pyramids," *Egypt. J. Remote Sens. Sp. Sci.*, vol. 24, no. 2, 2021, doi: 10.1016/j.ejrs.2020.12.006.

[14] L. Polidori and M. El Hage, "Methods : A Critical Review," *Remote Sens.*, vol. 12, no. 21, 2020.

[15] D. G. Habte, S. Belliethathan, and T. Ayenew, "Evaluation of the status of land use/land cover change using remote sensing and GIS in Jewha Watershed, Northeastern Ethiopia," *SN Appl. Sci.*, vol. 3, no. 4, 2021, doi: 10.1007/s42452-021-04498-4.

[16] M. E. D. Chaves, M. C. A. Picoli, and I. D. Sanches, "Recent applications of Landsat 8/OLI and Sentinel-2/MSI for land use and land cover mapping: A systematic review," *Remote Sensing*, vol. 12, no. 18. 2020, doi: 10.3390/rs12183062.

[17] B. Chatenoux *et al.*, "The Swiss data cube, analysis ready data archive using earth observations of Switzerland," *Sci. Data*, vol. 8, no. 1, 2021, doi: 10.1038/s41597-021-01076-6.

[18] M. D. Nguyen, O. M. Baez-Villanueva, D. D. Bui, P. T. Nguyen, and L. Ribbe, "Harmonization of landsat and sentinel 2 for crop monitoring in drought prone areas: Case studies of Ninh Thuan (Vietnam) and Bekaa (Lebanon)," *Remote Sens.*, vol. 12, no. 2, 2020, doi: 10.3390/rs12020281.

[19] R. S. Reddy, "Landsat-8 vs. Sentinel-2: Landuse Landcover Change Analysis and Differences in Gudur Municipality," *Int. J. Res. Appl. Sci. Eng. Technol.*, vol. 9, no. VI, 2021, doi: 10.22214/ijraset.2021.32711.

[20] M. Mathewos, S. M. Lencha, and M. Tsegaye, "Land Use and Land Cover Change Assessment and Future Predictions in the Matenchose Watershed, Rift Valley Basin, Using CA-Markov Simulation," *Land*, vol. 11, no. 10, 2022, doi: 10.3390/land11101632.

[21] A. Herawan, A. Julzarika, P. R. Hakim, and E. A. Anggari, "Object-Based on Land Cover Classification on LAPAN-A3 Satellite Imagery Using Tree Algorithm (Case Study: Rote Island)," *Int. J. Adv. Sci. Eng. Inf. Technol.*, vol. 11, no. 6, pp. 2254–2260, 2021, doi: 10.18517/ijaseit.11.6.14200.

[22] A. H. Syafrudin, S. Salaswati, and W. Hasbi, "Pre-Flight Radiometric Model of Linear Imager on LAPAN-IPB Satellite," in *IOP Conference Series: Earth and Environmental Science*, 2018, vol. 149, no. 1, doi: 10.1088/1755-1315/149/1/012068.

[23] P. R. Hakim, A. H. Syafrudin, S. Salaswati, S. Utama, and W. Hasbi, "Development of Systematic Image Preprocessing of LAPAN-A3/IPB Multispectral Images," *Int. J. Adv. Stud. Comput. Sci. Eng.*, vol. 7, no. 10, pp. 9–18, 2019.

[24] S. Utama, M. A. Saifudin, and M. Mukhayadi, "Momentum Biased Performance of LAPAN-A3 Satellite for Multispectral Pushbroom Imager Operation," in *IOP Conference Series: Earth and Environmental Science*, 2018, vol. 149, no. 1, doi: 10.1088/1755-1315/149/1/012062.

[25] B. Moradi, M. J. V. Zoej, S. Yaghoobi, and S. Yavari, "An improved approach based on terraindependent mathematical models for georeferencing pushbroom satellite images," *Photogramm. Eng. Remote Sensing*, vol. 87, no. 1, 2021, doi: 10.14358/PERS.87.1.53.

[26] S. Liang, J. Cheng, and J. Zhang, "Maximum likelihood classification of soil remote sensing image based on deep learning," *Earth Sci. Res. J.*, vol. 24, no. 3, 2020, doi: 10.15446/esrj.v24n3.89750.

[27] A. Kumar, R. D. Garg, P. Singh, A. Shankar, S. R. Nayak, and M. Diwakar, "Monitoring the Land Use, Land Cover Changes of Roorkee Region (Uttarakhand, India) Using Machine Learning Techniques," *Int. J. Soc. Ecol. Sustain. Dev.*, vol. 14, no. 1, 2023, doi: 10.4018/IJSESD.316883.

[28] L. M. Western, J. C. Rougier, I. M. Watson, and P. N. Francis, "Evaluating nonlinear maximum likelihood optimal estimation uncertainty in cloud and aerosol remote sensing," *Atmos. Sci. Lett.*, vol. 21, no. 8, 2020, doi: 10.1002/asl.980.

[29] A. H. Chughtai, H. Abbasi, and I. R. Karas, "A review on change detection method and accuracy assessment for land use land cover," *Remote Sens. Appl. Soc. Environ.*, vol. 22, 2021, doi: 10.1016/j.rsase.2021.100482.

[30] S. Dong, Z. Chen, B. Gao, H. Guo, D. Sun, and Y. Pan, "Stratified even sampling method for accuracy assessment of land use/land cover classification: a case study of Beijing, China," *Int. J. Remote Sens.*, vol. 41, no. 16, 2020, doi: 10.1080/01431161.2020.1739349.

[31] M. D. K. L. Gunathilaka and S. L. J. Fernando, "Accuracy Assessment of Unsupervised Land Use and Land Cover Classification Using Remote Sensing and Geographical Information Systems," *Int. J. Environ. Eng. Educ.*, vol. 4, no. 3, 2022, doi: 10.55151/ijeedu.v4i3.73.

[32] M. F. Baig, M. R. U. Mustafa, I. Baig, H. B. Takaijudin, and M. T. Zeshan, "Assessment of Land Use Land Cover Changes and Future Predictions Using CA-ANN Simulation for Selangor, Malaysia," *Water (Switzerland)*, vol. 14, no. 3, 2022, doi: 10.3390/w14030402.

[33] E. Duku, P. A. D. Mattah, and D. B. Angnuureng, "Assessment of land use/land cover change and morphometric parameters in the keta lagoon complex ramsar site, ghana," *Water (Switzerland)*, vol. 13, no. 18, 2021, doi: 10.3390/w13182537.

[34] M. Traore, M. S. Lee, A. Rasul, and A. Balew, "Assessment of land use/land cover changes and their impacts on land surface temperature in Bangui (the capital of Central African Republic)," *Environ. Challenges*, vol. 4, 2021, doi: 10.1016/j.envc.2021.100114.

[35] D. Phiri, M. Simwanda, S. Salekin, V. R. Nyirenda, Y. Murayama, and M. Ranagalage, "Sentinel-2 data for land cover/use mapping: A review," *Remote Sensing*, vol. 12, no. 14. 2020, doi: 10.3390/rs12142291.

[36] V. K. Mishra and T. Pant, "Open surface water index: a novel approach for surface water mapping and extraction using multispectral and multisensory data," *Remote Sens. Lett.*, vol. 11, no. 11, 2020, doi: 10.1080/2150704X.2020.1804085.

[37] P. Amatya, D. Kirschbaum, T. Stanley, and H. Tanyas, "Landslide mapping using object-based image analysis and open source tools," *Eng. Geol.*, vol. 282, 2021, doi: 10.1016/j.enggeo.2021.106000.

[38] Z. Deng and B. Quan, "Intensity Analysis to Communicate Detailed Detection of Land Use and Land Cover Change in Chang-Zhu-Tan Metropolitan Region, China," *Forests*, vol. 14, no. 5, 2023, doi: 10.3390/f14050939.

[39] T. Liu, L. Yang, and D. Lunga, "Change detection using deep learning approach with object-based image analysis," *Remote Sens. Environ.*, vol. 256, 2021, doi: 10.1016/j.rse.2021.112308.

[40] P. Potapov *et al.*, "Landsat analysis ready data for global land cover and land cover change mapping," *Remote Sens.*, vol. 12, no. 3, 2020, doi: 10.3390/rs12030426.

[41] W. Wu *et al.*, "New Scheme for Impervious Surface Area Mapping from SAR Images with Auxiliary User-Generated Content," *IEEE J. Sel. Top. Appl. Earth Obs. Remote Sens.*, vol. 13, 2020, doi: 10.1109/JSTARS.2020.3027507.

[42] F. Shi and M. Li, "Assessing land cover and ecological quality changes under the new-type urbanization from multi-source remote sensing," *Sustain.*, vol. 13, no. 21, 2021, doi: 10.3390/su132111979.

[43] H. Zheng and H. Li, "Spatial–temporal evolution characteristics of land use and habitat quality in Shandong Province, China," *Sci. Rep.*, vol. 12, no. 1, 2022, doi: 10.1038/s41598-022-19493-x.

[44] J. T. Nugroho, Z. Zylshal, and D. Kushardono, "LAPAN-A3 Satellite Data Analysis for Land Cover Classification (Case Study: Toba Lake Area, North Sumatra)," *Int. J. Remote Sens. Earth Sci.*, vol. 15, no. 1, 2018, doi: 10.30536/j.ijreses.2018.v15.a2782.